

## 1,4-Phenylene-bridged Subporphyrin–Porphyrin Dyad, Triad, and Tetrad

Yasuhide Inokuma, Shin-ya Hayashi, and Atsuhiko Osuka\*

Department of Chemistry, Graduate School of Science, Kyoto University, Sakyo-ku, Kyoto 606-8502

(Received December 15, 2008; CL-081164; E-mail: osuka@kuchem.kyoto-u.ac.jp)

1,4-Phenylene-bridged subporphyrin–porphyrin hybrid molecules were prepared by the Suzuki–Miyaura cross coupling reaction of *meso*-(4-bromophenyl)-substituted subporphyrin **2** and 5-pinacolboranyl porphyrin **3**. In all hybrid models examined, intramolecular energy transfer from the subporphyrin moiety to the porphyrin moieties proceeds efficiently.

Since our discovery of tribenzosubporphine in 2006,<sup>1</sup> subporphyrin, a genuine contracted porphyrin with a bowl-shaped 14 $\pi$ -aromatic circuit, has gathered much attention as a new class of visible-fluorescent chromophore, unique triangular bowl-shaped molecule, and boron-chelating supramolecular assembly.<sup>2,3</sup> One of the most significant characteristics of subporphyrin is the large *meso* substituent effects on the electronic properties of subporphyrin core, which is attributed to the low rotational energy barrier of *meso*-aryl groups.<sup>3c</sup> In this regard, a variety of *meso*-aryl-substituted subporphyrins have been explored so far. For example, intramolecular charge-transfer interactions in *meso*-(4-nitrophenyl)- or (4-aminophenyl)-substituted subporphyrins cause drastic alterations of absorption and fluorescence properties.<sup>3c,4</sup> Oligo(1,4-phenyleneethynylene)-substituted subporphyrins exhibit progressive increases in the absorption coefficients, fluorescence quantum yields, and two-photon absorption cross sections.<sup>5</sup> Furthermore, significant interchromophore interactions between two subporphyrin cores have been disclosed for a 4,4'-biphenylene-linked subporphyrin dimer.<sup>6</sup> The fluorescence of *meso*-phenyl-subporphyrin **1** is observed in a range of 500–600 nm and nicely matches with the Q-band absorption of porphyrin. This situation will allow an efficient energy transfer from subporphyrin to porphyrin in covalently-linked models. In this context, phenylene-bridged subporphyrin–porphyrin hybrids **4–7** were synthesized and their optical and electrochemical properties were investigated.

*meso*-Tri(4-bromophenyl)subporphyrin **2** and 5-pinacolboranylporphyrin **3** were coupled in the presence of a Pd-catalyst under standard Suzuki–Miyaura cross coupling conditions. Subsequent reduction of unreacted bromo groups afforded 1,4-phenylene-bridged subporphyrin–porphyrin dyad **4**, triad **5**, and tetrad **6** in 18, 19, and 7% yields, respectively, for two steps (Chart 1). The <sup>1</sup>H NMR spectrum of **4** shows C<sub>s</sub> symmetric features by showing four doublets at 9.43, 9.26, 9.13, and 9.10 ppm due to the porphyrin  $\beta$ -protons, and a couple of doublets and a singlet at 8.52, 8.30, and 8.19 ppm due to the subporphyrin  $\beta$ -protons. Observation of the protons of the 1,4-phenylene bridge as a pair of doublets indicates its free rotation with respect to the subporphyrin core. A similar <sup>1</sup>H NMR spectral pattern was recorded for **5**. On the other hand, the <sup>1</sup>H NMR spectrum of **6** exhibits C<sub>3</sub> symmetric features by displaying a singlet at 8.73 ppm due to the six  $\beta$ -protons of subporphyrin. 1,3-Phenylene linked subporphyrin–porphyrin dyad **7** was also prepared by a similar method.<sup>3d</sup>

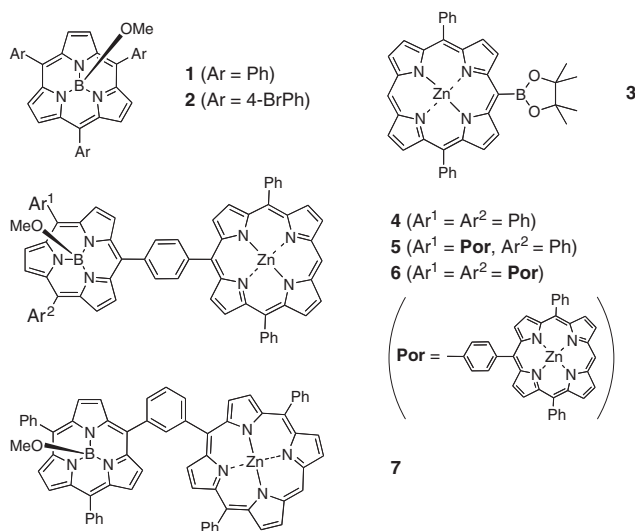
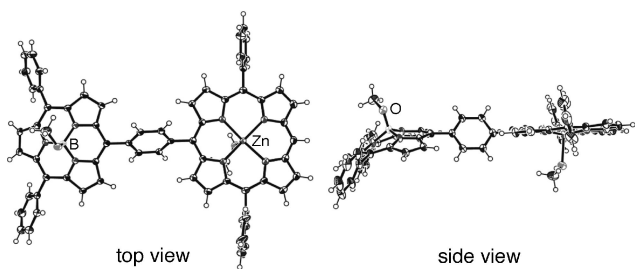
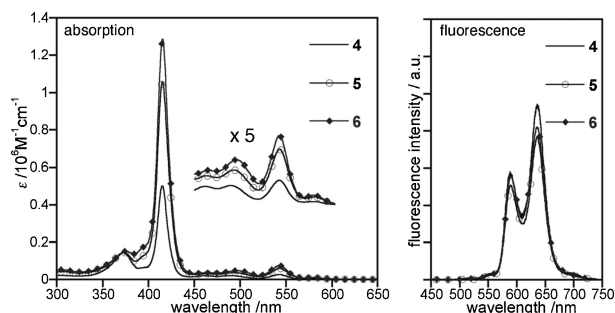


Chart 1.

Figure 1. X-ray crystal structure of dyad **4**.

A single crystal of dyad **4** suitable for X-ray diffraction analysis was grown from a mixture of CH<sub>2</sub>Cl<sub>2</sub>/MeOH. The solid-state structure of **4** shows a rather coplanar conformation with a small dihedral angle (16°) between the mean planes of porphyrin and subporphyrin, which are respectively tilted by 51.0 and 62.7° towards the 1,4-phenylene bridge (Figure 1).<sup>8</sup> The distance between the boron and zinc ions is 12.2 Å. The central Zn<sup>II</sup> ion in the porphyrin unit is apically coordinated by a methanol molecule.

Figure 2 shows absorption and fluorescence spectra of **4–6**. The absorption spectrum of **4** exhibits porphyrin-based Soret and Q-bands at 415 and 543 nm along with those of subporphyrin at 373 and 490 nm, which can be almost reproducibly by a linear combination of the absorption spectra of the fragment components. In the absorption spectra of **5** and **6**, the relative intensities of the porphyrin-based bands are increased and the subporphyrin-based Soret-like bands undergo slight but significant broadening, and the subporphyrin-based Q(0,0) band is progressively red-shifted in the order of **4** (490 nm) < **5** (494 nm) < **6** (496 nm). Fluorescence spectra of **4–7** were recorded by excita-



**Figure 2.** UV-vis absorption and fluorescence (dashed line;  $\lambda_{\text{ex}} = 373 \text{ nm}$ ) spectra of **4–6** in  $\text{CH}_2\text{Cl}_2$ .

tion at 373 nm, where the subporphyrin subunit is selectively excited. Interestingly, the fluorescence emission from the subporphyrin was completely quenched, and the fluorescence from the porphyrin only was observed at 598 and 636 nm. The fluorescence quantum yields are 3.4, 3.3, 3.3, and 2.6% for **4**, **5**, **6**, and **7**, respectively. The similar fluorescence spectra and quantum yields ( $\Phi_{\text{F}} = 3.1, 2.9, 3.0, \text{ and } 2.3\%$  for **4**, **5**, **6**, and **7**; Supporting Information; SI)<sup>9</sup> were also recorded upon excitation at 415 nm, where the porphyrin units are dominantly excited. The fluorescence excitation spectra of **4–7** detected at 640 nm were almost identical to the absorption spectra, indicating the quantitative energy transfer from subporphyrin to porphyrin. In sharp contrast, a 1:1 mixture of subporphyrin **1** and (5,15-diphenylporphyrinato)zinc(II) ( $2.0 \times 10^{-6} \text{ M}$  each) exhibited different fluorescence depending upon excitation wavelength, green fluorescence at 514 nm for excitation at 373 nm and red fluorescence at 630 nm for excitation at 408 nm, indicating inefficient intermolecular energy transfer at this concentration.

Oxidation potentials of **4–6** were measured by cyclic voltammetry in  $\text{CH}_2\text{Cl}_2$  containing 0.10 M  $\text{Bu}_4\text{NPF}_6$  as a supporting electrolyte. Under similar conditions, the reference molecules, **1** and ZnTPP,<sup>10</sup> exhibit the oxidation potentials at 0.71 V and at 0.42 and 0.71 V (vs. ferrocene/ferrocenium pair), respectively. Three reversible oxidation waves were observed at 0.36, 0.70, and 0.88 V for **4** and 0.34, 0.74, and 0.92 V for **5**. In the case of **6**, two reversible oxidation waves were at 0.39 and 0.75 V<sup>11</sup> (SI). These results indicate that subporphyrin and porphyrin segments retain their individual electrochemical characters but the covalent linkages of these electron-deficient segments and the generation of cationic sites lead to slight positive shifts of the oxidation potentials.

In order to understand the optical and electrochemical characteristics of these hybrid compounds, DFT calculation of **4** was performed at the B3LYP/6-31G\* level (SI). The calculation results show that LUMO and LUMO+1 are almost localized at the porphyrin segment and LUMO+2 and LUMO+3 are localized at the subporphyrin segment. Slight but distinct orbital interactions through a 1,4-phenylene bridge are observed for HOMO and HOMO–1, although the former is dominated at the porphyrin and the latter is dominated at the subporphyrin segment, respectively. As a consequence, HOMO–1 of **4**, which corresponds to subporphyrin  $a_1$ -orbital, undergoes remarkable stabilization compared to that of **1**. On the other hand, the energy level

of HOMO of **4** is by chance similar to that of ZnTPP. These results are in good agreement with the observed oxidation potentials, in that the first and second oxidation waves comparable to those of ZnTPP are assignable to the oxidation processes of the porphyrin segment and the third one at 0.88 V is assignable to the first oxidation of the subporphyrin site. Briefly, the porphyrin segment in **4** serves as an electron-withdrawing substituent for the subporphyrin subunit, but the electronic interactions are weak due to the orthogonal conformation of the 1,4-phenylene bridge to the porphyrin segment.

In conclusion, we prepared hybrids **4–7** as the first examples of covalently linked subporphyrin–porphyrin models by the Suzuki–Miyaura cross coupling reaction. Efficient intramolecular energy transfer from subporphyrin to porphyrin subunit was observed for **4–6**. Examination of further detailed of these hybrid systems is actively in progress in our laboratory.

This work was supported by a Grant-in-Aid (A) (No. 19205006) for Scientific Research from MEXT. Y. I. thanks the JSPS Research Fellowship for Young Scientists.

#### References and Notes

- 1 Y. Inokuma, J. H. Kwon, T. K. Ahn, M.-C. Yoo, D. Kim, A. Osuka, *Angew. Chem., Int. Ed.* **2006**, *45*, 961.
- 2 a) T. Torres, *Angew. Chem., Int. Ed.* **2006**, *45*, 2834. b) Y. Inokuma, A. Osuka, *Dalton Trans.* **2008**, 2517.
- 3 a) N. Kobayashi, Y. Takeuchi, A. Matsuda, *Angew. Chem., Int. Ed.* **2007**, *46*, 758. b) Y. Takeuchi, A. Matsuda, N. Kobayashi, *J. Am. Chem. Soc.* **2007**, *129*, 8271. c) Y. Inokuma, Z. S. Yoon, D. Kim, A. Osuka, *J. Am. Chem. Soc.* **2007**, *129*, 4747. d) Y. Inokuma, A. Osuka, *Chem. Commun.* **2007**, 2938. e) E. Tsurumaki, S. Saito, K. S. Kim, J. M. Lim, Y. Inokuma, D. Kim, A. Osuka, *J. Am. Chem. Soc.* **2008**, *130*, 438. f) S. Saito, K. S. Kim, Z. S. Yoon, D. Kim, A. Osuka, *Angew. Chem., Int. Ed.* **2007**, *46*, 5591.
- 4 Y. Inokuma, S. Easwaramoorthi, Z. S. Yoon, D. Kim, A. Osuka, *J. Am. Chem. Soc.* **2008**, *130*, 12234.
- 5 Y. Inokuma, S. Easwaramoorthi, S. Y. Jang, K. S. Kim, D. Kim, A. Osuka, *Angew. Chem., Int. Ed.* **2008**, *47*, 4840.
- 6 Y. Inokuma, A. Osuka, *Org. Lett.* **2008**, *10*, 5561.
- 7 A. G. Hyslop, M. A. Kellett, P. M. Iovine, M. J. Therien, *J. Am. Chem. Soc.* **1998**, *120*, 12676.
- 8 Crystallographic data for **4**:  $\text{C}_{67}\text{H}_{46}\text{BN}_7\text{O}_2\text{Zn}$ ,  $M_r = 1057.29$ , orthorhombic, space group  $Pbca$ ,  $a = 18.861(3) \text{ \AA}$ ,  $b = 20.114(3) \text{ \AA}$ ,  $c = 26.675(5) \text{ \AA}$ ,  $V = 10120(3) \text{ \AA}^3$ ,  $T = 123 \text{ K}$ ,  $Z = 8$ ,  $\mu(\text{Mo K}\alpha) = 0.543 \text{ mm}^{-1}$ ,  $D_{\text{calcd}} = 1.388 \text{ g/cm}^3$ , 11582 reflections measured, 8240 unique ( $R_{\text{int}} = 0.109$ ),  $R_1 = 0.0551$  ( $I > 2\sigma(I)$ ),  $R_w = 0.1497$  (all data), CCDC-711435.
- 9 Supporting Information is available electronically on the CSJ-Journal Web site, <http://www.csj.jp/journals/chem-lett/index.html>.
- 10 N. Armaroli, F. Diederich, L. Echegoyen, T. Habicher, L. Flamigni, G. Marconi, J.-F. Nierengarten, *New J. Chem.* **1999**, 77.
- 11 In differential pulse voltammetry (DPV) measurement, the third oxidation wave of **6** was observed at 0.99 V (see Figure S2 in SI).